



Cite this: *Environ. Sci.: Atmos.*, 2024, 4, 1170

Evaluating the potential secondary contribution of photosensitized chemistry to OH production in aqueous aerosols†

Emma A. Petersen-Sonn,^a Marcello Brigante,^b Laurent Deguillaume,^{cd} Jean-Luc Jaffrezo,^e Sébastien Perrier^a and Christian George^{id}*^a

This study explores the potential contribution of secondary production of OH radicals in aerosols and cloud/fog conditions arising from brown carbon (BrC) triplet state chemistry. For this purpose, extracts of brown carbon from atmospheric aerosols from Grenoble, France, were analyzed for their ability to produce triplet states from the degradation of a common triplet state probe, 2,4,6-trimethylphenol (TMP). This ability of brown carbon to produce triplet states was compared to that of three photosensitizers, where it was found that vanillin (VL) showed a similar rate of degradation of the probe and was hence chosen as an alternative to BrC in aqueous aerosols to investigate OH formation from triplet states. The rates of OH formation from the triplet states were compared to those from nitrate anions (NO_3^-) and hydrogen peroxide (H_2O_2), which are well-known sources of OH radicals in the aqueous phase, and a species that is structurally similar to VL, 4-hydroxybenzaldehyde (4HB). VL and 4HB both showed a 1–2 orders of magnitude higher rate of secondary OH formation than NO_3^- , while it was similar or one order of magnitude smaller than H_2O_2 . To evaluate the influence of the different OH radical sources in aqueous aerosols and cloud/fog conditions, the concentrations of the species were summarized from the literature. Considering the concentrations of HULISs in aerosols, the rates of secondary OH formation from BrC triplet states could potentially represent a significant source of OH in the atmospheric aqueous phase under some circumstances. This study shows the relevance of further investigations into the role of triplet states in impacting atmospheric oxidative capacity and studying other effects of triplet states in aerosols, a field that is, until now, still not fully understood.

Received 23rd July 2024
Accepted 20th August 2024

DOI: 10.1039/d4ea00103f

rsc.li/esatmospheres

Environmental significance

OH radicals drive the oxidation of organic matter in the aqueous phase of aerosols. Therefore, understanding how OH radicals are formed in aerosols is crucial for the estimation and calculation of oxidative reactions. Previous studies have shown OH formation from organic matter in surface waters and a few from organic species in aerosols. Herein, using and validating a single molecule photosensitizer, we explore secondary OH formation from the mentioned sources and compare it in the aqueous phase with several other sources. Finally, this study indicates that OH radical formation from excited triplet states might be highly influential in aqueous aerosols, and this chemistry should be further studied to understand its full impact.

^aUniversité Claude Bernard Lyon 1, CNRS, IRCELYON, UMR 5256, Villeurbanne, F-69100, France. E-mail: christian.george@ircelyon.univ-lyon1.fr

^bUniversité Clermont Auvergne, CNRS, Institut de Chimie de Clermont-Ferrand, F-63000, Clermont-Ferrand, France

^cUniversité Clermont Auvergne, CNRS, Laboratoire de Météorologie Physique, Clermont-Ferrand, France

^dUniversité Clermont Auvergne, CNRS, Observatoire de Physique du Globe de Clermont Ferrand, Clermont-Ferrand, France

^eUniversité Grenoble Alpes, CNRS, IRD, Grenoble INP, INRAE, Institut des Géosciences de l'Environnement, Grenoble, 38400, France

† Electronic supplementary information (ESI) available: Supporting Information (PDF), including additional information about the measurement of OH radical formation, extraction protocol for the aerosol samples, description of UPLC/UV methods for detecting trimethylphenol (TMP), literature studies on the concentrations of NO_3^- , H_2O_2 , HULIS, and phenols/nitrophenols in aerosols and/or cloud/fog conditions, and a comparison of previously measured OH formation rates in the literature. See DOI: <https://doi.org/10.1039/d4ea00103f>

1 Introduction

In recent years, attention has been focused on the presence of triplet states in aerosols.^{1,2} Triplet states have been shown to be important because of their ability to produce singlet oxygen^{3–7} and to degrade organic species.⁸ However, the chemistry behind these triplet states is still not fully known, and therefore, it is difficult to perceive the real extent of their impact in the aqueous aerosol environment, *i.e.*, deliquescent aerosols or in cloud/fog conditions. However, recent studies have examined the oxidizing ability of triplet states^{9–12} towards targeted organic compounds, mainly in surface waters. They found that the oxidizing ability of triplet states is comparable to that of the OH



radical, which is considered one of the most efficient oxidants in both gas and aqueous atmospheric phases.^{13,14}

With the evident importance of triplet states in surface waters, the question arises as to how large the influence of triplet states is in atmospheric waters. Triplet states have been found to degrade phenols, such as syringol, guaiacol, and phenol, while producing aqueous phase secondary organic aerosols (aqSOAs)^{15,16} at rates faster or similar to OH radicals.¹⁷ Triplet states were also investigated for their degradation of volatile organic compounds, where their rate constants were several orders of magnitude larger than those by singlet molecular oxygen.¹⁸ Other recent studies on triplet states showed their possible concentration in aerosols, highlighting the fact that they could be more abundant than OH radicals.^{19,20}

Indeed, a wide variety of molecules in particles can absorb light and enter an excited triplet state, and many of them share the existence of aromaticity, *e.g.*, one or more phenyl groups. A class of compounds where a large number of molecules possess these properties is brown carbon (BrC). However, the majority of reports in the literature on the concentrations of light-absorbing organic species focus on humic-like substances (HULISs), which is regarded as a subset of BrC. HULISs and BrC are not well-defined groups of compounds as many of their chemical properties vary greatly, depending on their origin and composition.²¹ Studies that have quantified HULISs in aerosols^{22–34} have found it in concentrations ranging from 9 (± 6) ngC m⁻³ (with a PM₁₀ concentration of 1.0 $\mu\text{g m}^{-3}$) in an Arctic site in Greenland³⁵ up to 8.28 $\mu\text{gC m}^{-3}$ (with a PM_{2.5} concentration of 69.7 $\mu\text{g m}^{-3}$) in a summer urban site in China;²⁵ in the aqueous aerosol phase, these concentrations would correspond to 1.1 M (Greenland, Arctic) and 14 M (China, urban). The conversion from $\mu\text{g m}^{-3}$ to M is described in the ESI.† The presence of high concentrations of these chromophores raises the question of their impact on the formation of OH in aqueous aerosols, though it has not yet been identified in full. In fact, it has been suggested that triplet state chemistry can be eventually regarded as a kind of catalytical cycle (see below),³⁶ where the chromophoric functionality inducing the triplet state is not consumed but regenerated in the presence of oxygen-producing as a side product HO_x (*i.e.*, OH and HO₂) radicals.

Investigations are therefore needed to understand whether triplet states indirectly produce OH radicals in significant amounts in aerosol and cloud/fog conditions and thereby induce even greater oxidizing effects than formerly predicted. Studies regarding the formation of OH in the aqueous phase mainly consider sources such as photolysis of nitrate/nitrite anions,^{37–40} hydrogen peroxide,^{41–43} and iron aqua-complexes.^{44–47} Other sources might also contribute significantly to the total OH concentration, such as the Fenton reaction.⁴⁸

Previous studies⁴⁹ have investigated the OH formation from organic matter (OM) in aerosols produced from seawater, with OH production rates of $(1.1\text{--}2.5) \times 10^{-8} \text{ M s}^{-1}$, while those of NO₃⁻ were $(1.4\text{--}1.9) \times 10^{-7} \text{ M s}^{-1}$. In a study by Anastasio *et al.* (2004)⁵⁰ regarding aerosols sampled in the Arctic, the authors found OH production rates of $2.78 \times 10^{-7} \text{ M s}^{-1}$, which they associated with the presence of unidentified chromophores in

the aerosol phase that showed great light absorption. Only 10% of the OH formation rate was attributed to NO₃⁻ photolysis. Sea-salt aerosols were also examined for their aqueous OH formation⁵¹ and showed rates of $9.44 \times 10^{-8} \text{ M s}^{-1}$, where NO₃⁻ was assumed to cause $59 \pm 25\%$ of the OH formation, while the authors pointed out that a large part of the unidentified other sources was likely to stem from organic matter. Also in fog waters, dissolved organic carbon has been observed to produce OH radicals.⁵² All of these studies point out an unknown pool of molecules, most probably organics like BrC, which are producing a large share of the OH in the aqueous systems.

Many studies that measured oxidants, such as triplet states, singlet oxygen and OH radicals in aerosols, focused on filter extraction performed in water.^{7,20,53} This allows for analysis of the majority of the water-soluble species in the collected particles, which includes both organic and inorganic parts of the particles. In contrast, during the study described below, the water-soluble fraction of brown carbon (BrC) was extracted for investigations focusing solely on the triplet states of this specific class of organic matter, minimizing (and eventually excluding) the contribution of other compounds. Facing the great molecular diversity of BrC and also the availability of samples, it is important to find proxies to help understand the chemistry of BrC in aerosols. Here, we compared photosensitizer proxies to collected ambient samples and found that, indeed, vanillin (VL) could be a reasonable proxy for BrC, as previously reported.^{54–63} In this contribution, we present an experimental investigation to assess the relative significance of secondary OH formation by triplet state chemistry (utilizing surrogates for aerosol and cloud/fog media) in comparison to well-established sources of OH in the atmospheric aqueous phase, such as nitrate and hydrogen peroxide.⁶⁴

2 Materials and methods

2.1 Chemicals

Chemicals used in the experiments included sodium nitrate (NaNO₃, >99%), hydrogen peroxide (30 w/w%), 4-benzoylbenzoic acid (4-BBA, 99%), 3-methoxy-4-hydroxybenzaldehyde (vanillin, VL, 99%), 2-hydroxyterephthalic acid (TAOH, 97%), and 2,4,6-trimethylphenol (TMP), which were obtained from Merck, and disodium terephthalate (TA, >99%), which was obtained from Alfa Aesar. Milli-Q water (18 M Ω cm) was used to prepare the solutions for the irradiation experiments.

2.2 Aerosol extracts

Total suspended particle (TSP) samples were collected in the winter of 2021/2022 on the roof (15 m above ground) of the Institut des Géosciences de l'Environnement (IGE) building on the campus of the University UGA in Grenoble (France). Two of these samples are referred to as 021 221 and 141 221 in this study (details of the samples are described in the ESI).† The sampler was a Tish Hivol working at 1.24 m³ h⁻¹ with 8 \times 10 inches quartz filters. The collection of aerosols was performed for 3 days to get enough organic matter for the experiments. During winter, the PM in the city is largely influenced by



domestic biomass burning emissions⁶⁵ and includes a large share of HULISs²² in organic matter. The BrC fraction is even larger, with many aromatics coming from this type of emission. There is also a large range of various organic acids from C2 to C7.⁶⁵ A chromatographic extraction of the filters was performed to obtain a large volume of a purified aqueous solution of BrC to conduct the experiments. The final solutions were analyzed for their DOC content using a TOC-L Shimadzu analyzer. The DOC content of the samples is given in the ESI.† The atmospheric samples were processed according to the protocols described in Baduel *et al.* 2009 & 2010,^{22,23} and hence, HULIS-type compounds were eluted and isolated from other atmospheric constituents prior to their use in the photochemical experiments. As a consequence, impurities or any interferences have little to no chance of influencing our results (due to the chromatographic separation steps).

2.2.1 Extraction protocol. The two samples, 021221 and 141221, were extracted for brown carbon (BrC) as follows. First, the filters were cut into pieces and placed in clean vials. Then, Milli-Q water was added to the vials (140 ml), and they were left shaking in the dark for 30 min. The content of the vials was extracted through a 0.45 μm acrodisc filter and retrieved in clean vials. Hereafter, the sample was acidified until it reached pH 2 using HCl solution. SPE OASIS cartridges were conditioned with methanol and water, and then the sample solution was let through, followed by 2 ml Milli-Q water to rinse. The cartridges were then quickly dried. The brown carbon was retrieved by letting 6 ml of methanol (2% ammonium) flow through. The solutions were dried under nitrogen, and finally, each sample was dissolved in 30 ml Milli-Q water. They were kept frozen and in the dark until use.

To determine the carbon content of the samples, a dissolved organic carbon (DOC) analysis was performed using a TOC-L Shimadzu analyzer (v. 1.08.00). For the automatic sampling, an OCT-L 8-port Shimadzu sampler was applied.

2.3 Detection of the triplet state probe

For the triplet state quantification, 2,4,6-trimethylphenol (TMP) was used as a well-known probe for excited triplet states.^{10,66–69} Solutions were all prepared with a concentration of 100 μM TMP. The aerosol samples had a concentration of 10 mgC L^{-1} . In the photosensitizer experiments, the concentration was 100 μM of the given photosensitizer.

The experiments were performed in a closed box, with a Xenon lamp mounted on top with a Pyrex filter. A cell of 50 ml was equipped with magnetic stirring and a cooling flow of water on the outside, keeping the temperature constant at 15 $^{\circ}\text{C}$. The solutions were irradiated for 120 min, during which sub-samples were withdrawn every 10–30 min. The experimental setup and UPLC methods are described in the ESI.†

The decrease in volume during the experiment is not considered to have a notable influence on the degradation of the probe due to the significantly larger volume of the solution (50 ml) compared to the samples that were removed (approximately 0.6 ml per sample).

2.4 Measurement of OH photogeneration rate

Measurements of OH in an aqueous solution were performed by applying a well-known probe, terephthalic acid (TA), a compound whose product from the reaction with OH, 2-hydroxyterephthalic acid (TAOH), is fluorescent. The OH sources investigated in this study do not interfere with the fluorescence from TAOH, and hence, the application of TA as a probe allows simple fluorescence measurements to track the OH formation with time. This probe has been used in various studies^{70–77} because of its selectivity and sensitivity towards OH. For OH radical detection, a different irradiation setup was employed. The solutions were placed inside a 10 mm quartz cell and irradiated by a 150 W Xenon lamp (LOT LSE140/160.25C) equipped with a liquid optical filter (filled with water) to remove heat from IR radiation and a Pyrex filter. The lamp was placed 30 cm away from the cell, thereby ensuring that the whole surface of the cell was illuminated. The temperature in the room was kept constant at 22 $^{\circ}\text{C}$. Solutions regarding the measurement of OH radicals were prepared with a concentration of 100 μM TA, while the concentrations of compounds producing OH (VL, NO_3^- , or H_2O_2) were varied. Fig. S7† shows the molar absorption coefficients of VL, 4HB, and TA, as well as the emission spectrum of the adopted irradiation system.

Fluorescence spectra were recorded every 5–10 min during 40–60 minutes of irradiation. By applying the TAOH calibration curves, it was possible to follow the formation of TAOH with time. Linear regressions were performed on these curves to obtain the rate of TAOH formation derived from the slope. Multiple experiments were performed to obtain the OH formation rates for varying concentrations of each compound producing OH. This gave rise to the total OH formation that is dependent on the concentration of the given compound.

3 Results and discussion

The optical characteristics of the ambient samples are shown in Fig. 1. The two samples are collected within a short time frame and are, therefore, expected to have similar fluorescence and absorption features. The fluorescence spectra for both samples show two main peaks with $\lambda_{\text{ex/em}} = 225/410$ and $325/414$ nm, with little difference in the intensity of these peaks. Fluorescence peaks at these positions have previously been identified as fluorescent signals originating from humic and fulvic acid-like species^{78–81} both for dissolved organic matter in surface waters and aerosol extracts of organic matter. In addition, a smaller peak is present at $\lambda_{\text{ex/em}} = 280/340$ nm, which, according to Wu *et al.*,⁸² could indicate marine humic-like organic matter. The UV-vis spectra of the samples likewise show similar spectra that appear featureless and show increasing absorbance with decreasing wavelength. The shape of the spectra is similar to other BrC spectra recorded previously.^{79,83} As this study focuses on the water-soluble extracts of BrC, there are undoubtedly sub-species of BrC that are not accounted for in these analyses. It has been suggested by other studies that the non-water-soluble fraction of BrC has increased



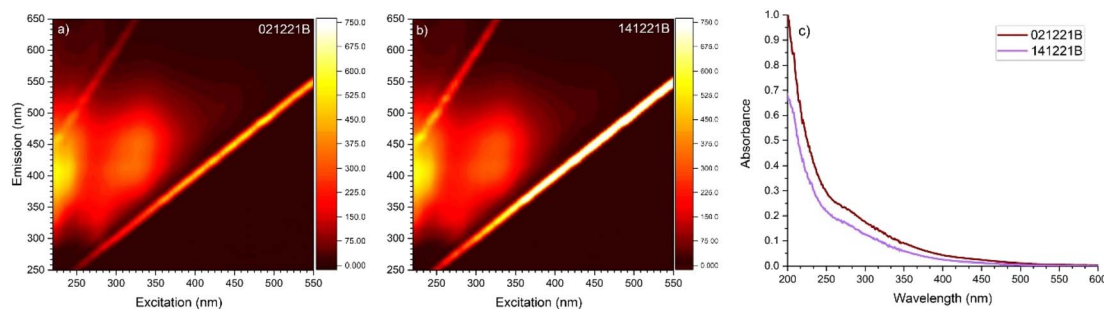
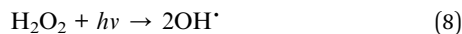
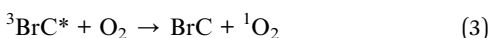
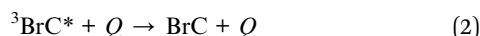
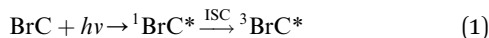


Fig. 1 Excitation emission matrix spectra of the two aerosol samples. (a) sample 021221B. (b) sample 141221B. (c) UV-vis absorption spectra of sample 021221B (dark red) and 141221B (purple).

absorbance compared to the water-soluble fraction, though the shape of the spectra does not change.⁸⁴

The brown carbon species responsible for this light absorption and fluorescence are expected to be able to enter a triplet state and have oxidizing abilities that might be competitive with OH radicals and singlet oxygen in atmospheric aerosols. The chemical reactions below show possible BrC photochemical reactions in an aqueous environment. Chromophores in BrC can undergo energy transfer to other compounds, such as molecular oxygen, thereby forming singlet oxygen ($^1\text{O}_2$). It can also be quenched by other compounds in the aqueous solution (Q) and return to their original state. Other commonly suggested pathways are hydrogen abstraction or electron transfer from/to a donor molecule (including self-reaction), inducing a cycle suggested to form OH radicals through HO_2 reactions.



The characterization of steady-state concentrations of excited triplet states of organic matter is mostly performed by applying a probe and measuring its decay by liquid chromatography with UV/vis detection. Here, we have chosen a common triplet state probe, 2,4,6-trimethylphenol (TMP). Through calculations using the first-order decay rate constant, as described in the ESI,[†] the estimated steady-state concentrations of triplet states of the brown carbon extracts are $(6.34 \pm 5.3) \times 10^{-14}$ and $(1.14 \pm 0.95) \times 10^{-13}$ M for the 021 221 and 141 221 samples, respectively. The large errors on these values are due to the error on the average of many rate constants

between triplet states and TMP that is used in the calculation (see Section S3[†]). The values are in good agreement with previous studies detecting triplet states from filter sampling, which have reported triplet state steady-state concentrations in the range of 1×10^{-14} to 9×10^{-13} M.^{20,85–87} By applying a chromatographic extraction method for the water-soluble brown carbon in this study, the degradation of the probe is considered to be mainly caused by BrC triplet states, with minimal influence from other water-soluble components of the filter samples in contrast to previous studies. However, it has recently been proposed in a comprehensive study of triplet state probes⁶⁹ that TMP might undergo inhibition from other components in particle extracts, such as other phenols, and return to its initial state, hereby causing less degradation. Therefore, in applying this probe to the chromatographic separated BrC fraction, the estimated steady-state triplet state concentrations are assumed to be underestimated.

It is well established that triplet states of organic matter can undergo energy transfer to molecular oxygen in solutions to form singlet molecular oxygen ($^1\text{O}_2$). In filter extracts from particulate matter, previous studies have measured the steady-state triplet state and singlet oxygen concentrations along with OH radical concentrations. The OH radicals formed in these solutions could have been formed through several pathways, such as from photolysis of hydrogen peroxide or nitrate/nitrite anions or from dark Fenton chemistry reactions. However, it is believed that the triplet states of organic matter, such as BrC, can likewise lead to hydroxyl radical formation in an aqueous solution, as described in chemical eqn (4)–(8).

Unfortunately, the TA probe cannot be directly used to determine the OH production from the fraction of BrC because of overlapping fluorescence from the various BrC species, as seen in Fig. S8.[†] Hence, it is difficult to determine an exact OH formation production rate from BrC, and this necessitates a BrC proxy for initial estimations of such a rate. Here, we tested three different photosensitizers, namely, 4-benzoylbenzoic acid (4-BBA), 3-methoxy-4-hydroxybenzaldehyde (vanillin, VL), and imidazole-2-carboxaldehyde (2-IC), for their degradation of TMP to compare with the two ambient aerosol samples.

Firstly, from Fig. 2, we observed that the rates of degradation of TMP between the ambient samples vary by almost a factor of 2, certainly reflecting atmospheric variability. From the slopes



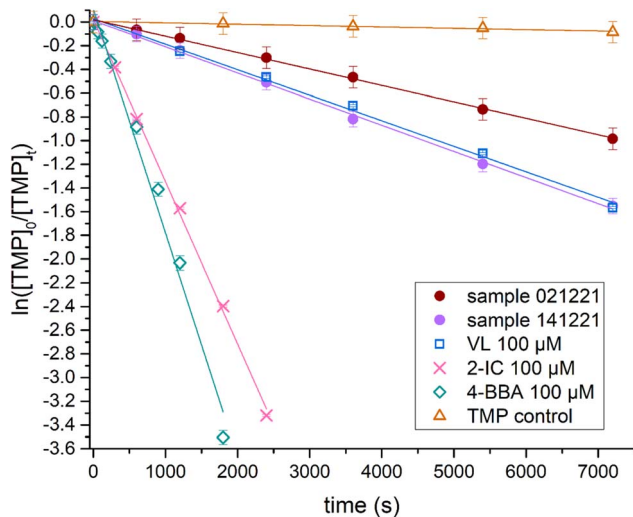


Fig. 2 Degradation of the triplet state probe, TMP, by two aerosol samples (021 221 and 141 221, 10 mgC L⁻¹) and three photosensitizers (VL, 2-IC, and 4-BBA). All experiments contained 100 μM TMP. The error bars represent the variation from the theoretical initial TMP concentration.

of the decay shown in Fig. 2, the rates were determined as (1.38 ± 0.021) and $(2.21 \pm 0.037) \times 10^{-4} \text{ s}^{-1}$ for the 021 221 and 141 221 samples, respectively. The variation in the amount of triplet states produced by the samples is expected to be caused by the difference in the sampling period, thereby resulting in a difference in composition. This is possibly related to the difference in absorbance of the two samples in the UV-vis spectra shown in Fig. 1c. For the selected photosensitizers, the measured decay rates were $(2.15 \pm 0.064) \times 10^{-4} \text{ s}^{-1}$, $(1.37 \pm 0.026) \times 10^{-3} \text{ s}^{-1}$, and $(1.89 \pm 0.088) \times 10^{-3} \text{ s}^{-1}$ for VL, 2-IC, and 4-BBA, respectively. The TMP control showed a rate of $(1.14 \pm 0.11) \times 10^{-5} \text{ s}^{-1}$. This corresponds to triplet state steady-state concentrations $(1.39 \pm 1.1) \times 10^{-13}$, $(9.31 \pm 7.5) \times 10^{-13}$, and $(1.29 \pm 1.0) \times 10^{-12} \text{ M}$ for VL, 2-IC, and 4-BBA, respectively.

It is clear that vanillin (VL) is the only one of the three photosensitizers that resembles the BrC samples in their degradation of TMP. The degradation of TMP by 4-BBA and 2-IC appears at a rate one order of magnitude larger than the ambient samples. This suggests that VL produces a similar amount of triplet states (although at different energies) and could be a proxy for the studied BrC fractions. In addition, the EEM spectra of the VL compare well to those of the ambient samples, as shown in the ESI.† This similarity could arise from the fact that these winter samples were impacted by biomass burning, while VL is a known tracer for such emissions.^{59–63} Further studies are warranted to fully evaluate how VL compares to other BrC samples from varying origins and seasons.

³VL* compares well to the ambient samples. It was hereafter investigated for its OH production rate and compared to two well-known photochemical sources of OH radicals, namely hydrogen peroxide and nitrate anions. To better characterize the OH formation from organic triplet states, the molecule 4-hydroxybenzaldehyde (4HB), a compound with a structure

similar to VL, was also investigated. All the OH formation rates were probed by the fluorescence of the molecule 2-hydroxyterephthalic acid, for which VL does not have a large overlap in contrast to the ambient samples.

3.1 OH production from photosensitizer molecules

The OH formation rates were calculated for nitrate anions, hydrogen peroxide, VL, and 4HB. The OH steady-state concentrations were also calculated and are shown in Table S2 and Fig. S3–S6.† Under our experimental conditions, the OH formation rates from NO_3^- and H_2O_2 were $(4.16 \pm 0.51) \times 10^{-7} \text{ M s}^{-1} \text{ M}(\text{NO}_3^-)^{-1}$ (Fig. S9†) and $(1.64 \pm 0.07) \times 10^{-5} \text{ M s}^{-1} \text{ M}(\text{H}_2\text{O}_2)^{-1}$ (Fig. S10†), respectively. Values for NO_3^- are in the same order of magnitude, and H_2O_2 values are one order higher than those reported in the literature.^{64,88–90} The discrepancy in H_2O_2 OH production rates compared to literature values could be attributed to the low H_2O_2 concentrations applied in the experiments in the previous studies (up to 40 μM in Mopper & Zhou, 1990). In our study, we applied larger concentrations to move toward aerosol-relevant hydrogen peroxide concentrations, which can be up to the mM range (see Table 1). The OH formation rate (normalized to the precursor concentration) from VL was $R_{\text{OH}} = (9.0 \pm 1.1) \times 10^{-6} \text{ M s}^{-1} \text{ M}(\text{VL})^{-1}$, while it was one order of magnitude smaller for 4HB, $R_{\text{OH}} = (9.2 \pm 0.28) \times 10^{-7} \text{ M s}^{-1} \text{ M}(\text{4HB})^{-1}$. These compounds were tested for concentrations between 5 and 100 μM, although they only showed a linear OH formation rate between 5 and 37.5 μM, while there was a decrease or a plateau in the OH formation rate with higher concentrations (see Fig. S11 and S12†). The reported rate is calculated from the linear regression between 5 and 37.5 μM, which is similar to concentrations of VL measured in biomass-burning aerosols.⁹¹ Both VL and 4HB showed R_{OH} that are within the ranges of the R_{OH} of nitrate and hydrogen peroxide and could thereby be considered atmospheric relevant if the concentrations of the species forming triplet states in aerosol or clouds are present in sufficient amounts.

The OH formation rates in the ranges investigated for the two photosensitizers were $3.4\text{--}5.9 \times 10^{-11}$ and $0.35\text{--}2.5 \times 10^{-10} \text{ M s}^{-1}$ for 4HB and VL, respectively. These are rates that are comparable to OH formation rates measured in previous studies (see Table S3†) for aerosols and cloud/fog waters that range between 10^{-12} to 10^{-6} M s^{-1} , where the cloud/fog values tend to be in the lower end of this range and the aerosol values in the higher end.

Choosing vanillin and 4-hydroxybenzaldehyde to estimate the OH production from triplet states that are present in aqueous aerosols cannot incorporate the large complexity that exists in the aerosols. Though it is not complete, we believe it is useful to estimate the importance of OH production from organic triplet state species. VL has absorbance well into the visible spectrum and might well represent BrC due to the amount of triplet states produced compared to aerosol sample extracts (Fig. 2), and it is also a compound that has been measured in aerosols and clouds/fogs. 4HB was chosen as a light-absorbing compound that might be present in clouds due to its similarity in structure to other phenols found in



Table 1 Range of aerosol and cloud/fog concentrations based on a selection of published data^a

	Aerosols (M)			Cloud/fog (M)
	Urban	Rural	BB ^b	Rural
NO ₃ ⁻	1.2–9.1	1.6 ^c –2.4	0.16–6.8	4.8×10^{-6} – 1.0×10^{-3}
H ₂ O ₂	0.25 – 1.8×10^{-2}	—	—	3.9×10^{-6} – 6.0×10^{-5}
HULIS (a)/(N)Phs (C/F)	4.1–14.7	7.3–8.3	4.9–9.6	3.6×10^{-10} – 1.53×10^{-6}

^a Unless otherwise stated, the aerosols are PM_{2.5}. HULISs are shown as a representative for triplet state sources in aerosol (a) and (N)Phs for cloud/fog (C/F) conditions. All references are listed in the ESI. ^b BB: biomass burning. ^c PM₁.

clouds. It also has a similar structure to VL and could thereby indicate how a small difference in the structure of the species (the absence of a methoxy-group) could influence the OH production from the triplet states of the molecule. Although, these species, *i.e.*, VL and 4HB, have some limitations. Firstly, both compounds show a non-linear OH production above 37 μM. Single molecules, such as VL and 4HB, might be observed in aerosols or clouds at concentrations of approximately 5–37 μM. Although, questions arise of whether other sources of triplet states show similar trends of plateaus at higher concentrations, leading to rates of OH production that cannot be linearly scaled to larger concentrations. Triplet state sources with distinct structural features need to be examined to evaluate how the OH production rates behave for other compounds. Secondly, 4HB only has a small absorbance at wavelengths longer than 350 nm and might not be considered a large contribution of the BrC in clouds/fogs. Even though the OH production from this compound shows that there is also a possible pool of triplet state species absorbing light in the 300 to 350 nm range, which might be influencing the OH production in clouds/fogs, though they are not absorbing much visible light.

Another factor that is not accounted for in the measurements of the OH formation rates is the degradation of the triplet state source. The OH production is assumed to be a catalytic cycle according to eqn (2)–(5), where the triplet state source (BrC) is brought back to its original state. Although, due to indications that the investigated species is possibly slightly degraded by either photolysis or reaction with OH radicals, it might not be a fully catalytic cycle. The second-order rate constant for OH with TA is $4.0 \times 10^9 \text{ M}^{-1} \text{ s}^{-1}$.⁶⁴ For VL and OH, the rate constant is estimated to be $4 \times 10^8 \text{ M}^{-1} \text{ s}^{-1}$.⁹² Hereby, VL can be expected to not have a large loss to OH reactions as it reacts with OH at about an order of magnitude slower than TA reacting with OH. A rate constant between 4HB and OH radicals was not found in the literature. Additionally, the linear regression that was made to obtain the OH formation rate was performed only in the range of 5 to 37.5 μM. Hereby, in the applied concentrations, the photosensitizers had at least a factor of 3 lower concentration than the probe ([TA] = 100 μM). Combined with a higher rate constant for TA compared to VL, this gives an uncertainty below 3% and hence is considered to be negligible. The quenching of triplet states by oxygen is also an important pathway to consider (see Fig. S2†). Naturally, oxygen dissolved

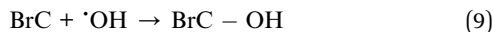
in the aqueous phase will interfere with the triplet states, such as by the formation of singlet oxygen.⁵³ However, the experiments in this study were performed with air-saturated solutions that we expect to have similar oxygen concentrations as atmospheric aerosols. In Fig. 2, aerosol samples that are extracted for BrC are analyzed for their degradation of TMP (*i.e.*, formation of triplet states) and are compared to that of VL. Here, a similar quenching of triplet states by the aerosol samples and VL is observed, and therefore, we might expect that VL triplet states are quenched in a similar way as other triplet state species in ambient aerosols.

From observations in the UV-vis absorption peaks, the decay of 4HB with increasing irradiation time can be observed in the UV-vis spectra shown in Fig. S21.† Since the solutions for the experiments contain both 4HB and TA, it is not possible to follow strictly the whole spectrum of 4HB, though TA does not have absorbance above 300 nm (see Fig. S7†). Therefore, the shoulder that is observed at 335 nm is attributed to 4HB only. With increasing irradiation time, this shoulder is observed to have decreasing absorbance, showing a decay of 4HB during the experiment. A similar observation is made for VL, where there is a decay of the VL peak at 310 nm. The decay of both compounds is approximately linear, and the first-order rates of decay of VL and 4HB are 7.59×10^{-5} and $1.8 \times 10^{-4} \text{ s}^{-1}$, respectively. These values suggest that 4HB either has a faster reaction with OH radicals or faster decay by photolysis than VL.

Another detail that arises from the absorbance spectra of 4HB is the formation of a new peak at 475 nm (see Fig. S22†). This peak appears after 20 min of irradiation, and even though the absorbance at the end of the experiment is quite low, this indicates the formation of species that absorb light in the visible range, suggesting further BrC formation from these reactions. VL likewise shows the formation of further BrC species, although the maximum of the peak of the formed BrC species is at longer wavelengths, at approximately 525 nm. The decay of the triplet state sources and the formation of new light-absorbing species is likely due to the reaction of OH radicals with VL or 4HB. Typically, these reactions involve the addition of OH radicals to the aromatic ring or the replacement of the ketone moiety with a carboxylic acid group.⁹²

Therefore, a chemical equation that could be useful to consider in connection with the previous eqn (1)–(8) is the reaction between OH and the proxies for the brown carbon species that gives a product, BrC–OH (eqn (9)).





The quantum yields calculated (shown in Section S10†) for the OH formation from the two photosensitizers were similar, (1.04 ± 0.020) and $(1.12 \pm 0.29) \times 10^{-4}$ for VL and 4HB, respectively. These values are comparable to those in previous studies, which found quantum yields of OH radicals between 1.3×10^{-5} and 1.0×10^{-2} for cloud water and extracts of aqueous aerosols.^{64,90,93,94}

Overall, VL was chosen as a proxy for aerosol samples because it showed a similar triplet state formation as the aerosol samples that were extracted for BrC, as seen in Fig. 2. It is, furthermore, a compound that has been observed in aerosol measurements^{95,96} and applied as a proxy in previous studies.^{97,98} 4HB was chosen to show further variability of the OH production from aromatic species.

3.2 Estimating OH formation rates in atmospheric conditions

To evaluate the possible influence of OH production from triplet states compared to nitrate anions and hydrogen peroxide photochemistry, it is necessary to consider the precursors' concentrations in aerosols and also cloud/fog environments. Then, the concentration normalized OH production rates reported above could be used to scale them to ambient conditions. Unfortunately, not many studies report BrC concentrations, though humic-like substances (HULISs) have been measured in various locations. HULISs are considered a subset of BrC, and therefore, are possibly an underestimation of the sources of triplet states in aerosol, though more field measurements of the full BrC pool are needed to have better estimations. The HULIS measurements have been summarized in Table 1, along with nitrate and hydrogen peroxide aerosol concentrations, while the full set of literature values is presented in the ESI.† The conversion from the unit $\mu\text{g m}^{-3}$, reported in the literature, to the unit mol L^{-1} is described in the ESI (Section 7).†

Even though HULISs and BrC might be present in clouds and fogs, they are scarcely measured in these environments. Another group of light-absorbing compounds in clouds/fogs with similar photochemical abilities as HULISs, or the mentioned photosensitizers, is nitrophenols and phenols ((N)Phs). These are (to some extent) more commonly detected in clouds/fog.⁹⁹ In an effort to best estimate triplet state concentrations, HULIS concentrations are shown for aerosols and (N)Ph concentrations for cloud/fog conditions. These values are presented in Table 1. Naturally, the concentrations of (N)Ph in clouds and fogs represent only a small fraction of the light-absorbing compounds present in these aqueous media. As mentioned previously, the carbonyl group on the aromatic ring is believed to be highly influential in the formation of triplet states, and it is possible that it is also driving the formation of OH radicals from triplet states. Therefore, the ideal concentrations to apply for these approximations are aromatic carbonyl species in the cloud/fog environments. Though these are very sparsely reported in the literature, (N)Ph concentrations are

used instead. Based on these concentrations, subsequent calculations to assess OH sources in cloud/fog are assumed to represent an underestimated assessment.

From Table 1, it is evident that the concentration of triplet state precursors in aerosols (HULIS) is comparable to the other OH sources, but in cloud/fog, the concentrations of the chosen proxy for triplet state sources ((N)Phs) are a great deal lower.

The range of concentrations in Table 1 was used to compare the overall rates of OH formation from the species investigated using the normalized OH formation rate previously measured for the species (concentration-dependent, in units of $\text{M s}^{-1} \text{M}(\text{COMP})^{-1}$) and assuming a linear relationship between the precursor concentration and the actual OH production rate (*i.e.*, without any screening effect for instance). This gave spans of overall OH formation rates (independent of species concentration), which are visualized in the boxplots for different conditions in Fig. 3, S13, and S14.† These rates are shown for nitrate, hydrogen peroxide, and triplet states (with these data using VL (and 4HB) as proxy). The rates of OH production from NO_3^- and H_2O_2 reported in previous studies are used together with the rates obtained in this study to expand the range of overall OH formation rates (in M s^{-1}) calculated for the boxplots. For the calculation of overall OH formation rates from triplet states, the boxplots show the R_{OH} from VL and from 4HB multiplied with the concentrations of either the HULIS or (N)Ph concentrations. With both of these photosensitizers, it is expected that a reasonable range of OH formation rates is reached. VL represents triplet states that are comparable to BrC in their steady-state concentrations, and 4HB represents an estimation of triplet states that are less efficient in producing OH (by one order of magnitude).

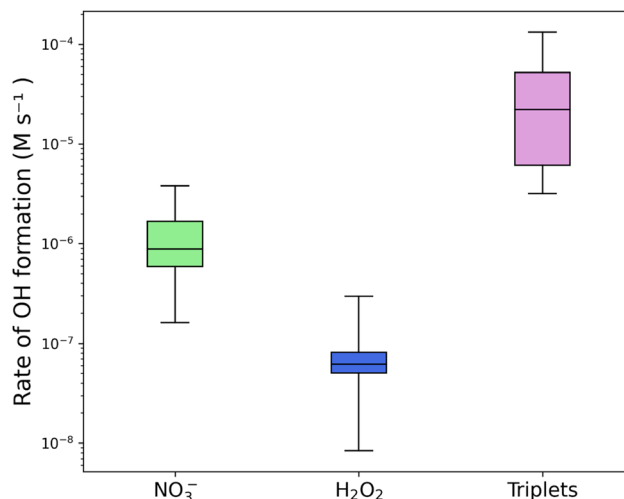


Fig. 3 Boxplots of rates of OH formation in urban aerosols of the investigated species. OH formation rates calculated in this study or reported in previous studies (for NO_3^- and H_2O_2) are multiplied by a range of concentrations of the species found in the literature. The minimum and maximum of the range of concentrations are shown in Table 1, and all the values and references can be found in Tables S4–S6.†



Fig. 3 shows the boxplot of the OH formation rate estimations under urban conditions, where the NO_3^- and H_2O_2 photoinduced formation rates of OH are 1–2 orders of magnitude smaller than values for the triplet state. In this plot, it is evident that the OH produced by triplet states is important in urban aerosols, illustrating that the OH formation from triplet states in aerosols could be as, or more, essential than the other large OH sources. It is possible that the OH production rates from H_2O_2 are also underestimated due to limited measurements in the aerosol aqueous phase. Nitrate anions are widely measured in aqueous aerosols, although most measurements are from locations in Asia, and the aerosol community would benefit from measurements on other continents to expand the knowledge.

For the cloud/fog conditions, shown in Fig. S13,† the OH production rates from triplet states (with the (N)Phs as proxy) appear much lower, and even negligible, compared to those of NO_3^- and H_2O_2 . This plot suggest that triplet states are not likely to be important sources of OH radicals in cloud/fog. As previously mentioned, the concentrations of triplet state sources in the cloud or fog water are not well quantified, and the rates of OH formation from triplet states in the environment are being underestimated due to a lack of measurement of light-absorbing compounds, such as (N)Ph or HULIS in cloud/fog. In the cloud/fog environment, the H_2O_2 concentrations are more defined than in aerosols. Nitrate anion concentrations are also well-defined in cloud/fog environments. In general, for both aerosol and cloud/fog, measurements of the mentioned species are primarily taken in three continents: Asia, Europe, and North America. Therefore, it would be beneficial for future studies to obtain information on the concentrations of these species in other parts of the world.

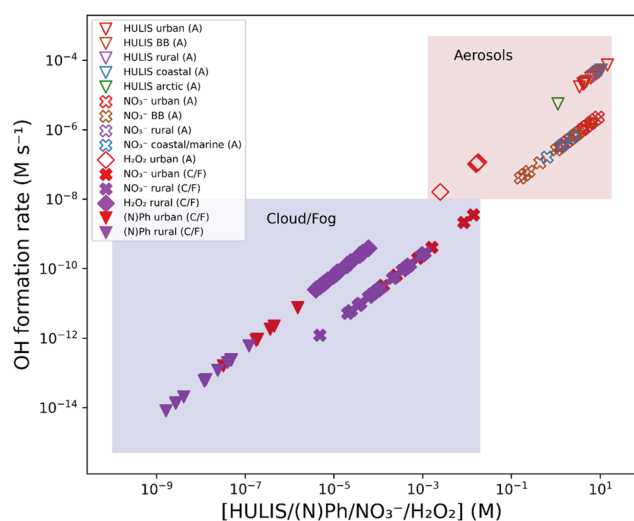


Fig. 4 Estimated OH formation rates for nitrate, hydrogen peroxide, and triplet state sources vs. the concentration. The OH formation rates are calculated using the literature values for concentrations in Tables S4–S9.† (A): aerosols. (C/F): cloud/fog. A zoomed-in aerosol region with nitrate and HULIS values is shown in Fig. S15.†

The boxplot in Fig. 3 shows the OH formation rate for one condition (urban aerosols), Fig. 4 shows the whole range of concentrations reported in the literature (x -axis), with the corresponding OH formation rates (y -axis) for all compounds and conditions that were investigated in this study. Bearing in mind the limits of the calculations, this aims to provide a simple (not to say simplistic) overview of the importance of the different species under various conditions. In this figure, the colored areas show how the OH formation rates are grouped into two regions: cloud/fog (purple) and aerosols (beige). The estimated triplet states, in the form of HULIS, are dominating in the aerosol region. The triplet states show larger OH formation rates than both nitrate and hydrogen peroxide in the full region of concentrations. However, in cloud/fog conditions, the influence of OH formation from triplet states is evaluated to be small. Reporting actual OH steady-state concentrations would require considering its various sinks, which are quite complex to estimate. Atmospheric aerosols vary in composition and also in concentration of the various species, which depend on numerous factors. This is why, in the following, the OH formation rates from various sources are intercompared.

As mentioned, an overview of OH formation rates measured in the atmosphere from a variety of sources is shown in Table S3† and covers aerosols, clouds and fogs at different locations. Naturally, there are numerous chemical species that could be triplet state sources and possibly produce OH radicals. It is difficult to know the effect of all of these because of the complexity of these compounds.

A group of complex species that is often found in surface waters is chromophoric dissolved organic matter (CDOM). As discussed by Chen *et al.* (2021),⁶⁸ different types of CDOM have different rates and abilities to generate triplet states, and thereby, it is not only dependent on the concentration of the source of triplet states but also the composition. The composition of aerosols and clouds naturally depends on the location, atmospheric dynamics, and seasonality. A study investigated the OH production inside the CDOM microphase,¹⁰⁰ *i.e.*, the “phase” that occurs within the CDOM molecules because of their large size and hydrophobic qualities. The authors found that compared to the aqueous OH, the concentration inside the CDOM microphase was $210 (\pm 31)$ fold increased, illustrating that a large amount of the OH formed from CDOM is likely to be produced inside the microphase of CDOM. If the same reactivity can be expected for chromophores in the aqueous aerosol environment, such as HULIS and BrC, the OH produced from excited triplet states would be even more influential in these conditions. Combined with the results from this study, it emphasizes the importance of investigating triplet states for their oxidative properties in the aqueous aerosol environment.

4 Conclusion

Here, we intend to provide some of the first indications as to how important the OH formation from excited triplet states in BrC aerosols could be. The rates of OH formation from excited triplet states were larger than from nitrate anions but below those of hydrogen peroxide, though when considering the



concentrations of possible triplet state sources in the aqueous aerosols, they represent the largest production of OH radicals, by a few orders of magnitude. The measurements in this study were performed solely in the aqueous phase. These results do not consider the intricate processes that could occur in the gas phase surrounding the aerosols, in the air–water interface, or in the potential microphase in large chromophoric triplet state sources. All of these processes could possibly have an effect on these OH formation rates. However, this study underlines the need for further research on the oxidative capacity of excited triplet states in the aqueous aerosol environment. The overview of literature values of concentrations of triplet state sources also necessitates a more comprehensive quantification of these to improve the estimation of the magnitude of triplet state produced OH in the atmosphere.

Data availability

All the data supporting this article have been included as part of the main text and in the ESI.†

Conflicts of interest

There are no conflicts to declare.

Acknowledgements

This work was supported by the French National Research Agency under grant agreement SENSOX (ANR-22-CE01-0023), the French national program LEFE/INSU through the project TRIPLET. JL Jaffrezo is very grateful to C Baduel for providing the protocol and tools for the atmospheric PM extraction of HULIS and BrC on the Air O Sol analytical platform of IGE.

References

- M. Schmitt, K. J. Moor, P. R. Erickson and K. McNeill, Sorbic Acid as a Triplet Probe: Reactivity of Oxidizing Triplets in Dissolved Organic Matter by Direct Observation of Aromatic Amine Oxidation, *Environ. Sci. Technol.*, 2019, **53**(14), 8087–8096, DOI: [10.1021/acs.est.9b01789](https://doi.org/10.1021/acs.est.9b01789).
- J. P. Bower and C. Anastasio, Degradation of Organic Pollutants in/on Snow and Ice by Singlet Molecular Oxygen (1O_2) and an Organic Triplet Excited State, *Environ. Sci.: Processes Impacts*, 2014, **16**(4), 748–756, DOI: [10.1039/C3EM00565H](https://doi.org/10.1039/C3EM00565H).
- C. A. Davis, K. McNeill and E. M.-L. Janssen, Non-Singlet Oxygen Kinetic Solvent Isotope Effects in Aquatic Photochemistry, *Environ. Sci. Technol.*, 2018, **52**(17), 9908–9916, DOI: [10.1021/acs.est.8b01512](https://doi.org/10.1021/acs.est.8b01512).
- P. R. Erickson, K. J. Moor, J. J. Werner, D. E. Latch, W. A. Arnold and K. McNeill, Singlet Oxygen Phosphorescence as a Probe for Triplet-State Dissolved Organic Matter Reactivity, *Environ. Sci. Technol.*, 2018, **52**(16), 9170–9178, DOI: [10.1021/acs.est.8b02379](https://doi.org/10.1021/acs.est.8b02379).
- K. J. Moor, M. Schmitt, P. R. Erickson and K. McNeill, Sorbic Acid as a Triplet Probe: Triplet Energy and Reactivity with Triplet-State Dissolved Organic Matter via ^{10}P Phosphorescence, *Environ. Sci. Technol.*, 2019, **53**(14), 8078–8086, DOI: [10.1021/acs.est.9b01787](https://doi.org/10.1021/acs.est.9b01787).
- S. Bogler, K. R. Daellenbach, D. M. Bell, A. S. H. Prévôt, I. El Haddad and N. Borduas-Dedekind, Singlet Oxygen Seasonality in Aqueous PM₁₀ Is Driven by Biomass Burning and Anthropogenic Secondary Organic Aerosol, *Environ. Sci. Technol.*, 2022, **56**(22), 15389–15397, DOI: [10.1021/acs.est.2c04554](https://doi.org/10.1021/acs.est.2c04554).
- A. Manfrin, S. A. Nizkorodov, K. T. Malecha, G. J. Getzinger, K. McNeill and N. Borduas-Dedekind, Reactive Oxygen Species Production from Secondary Organic Aerosols: The Importance of Singlet Oxygen, *Environ. Sci. Technol.*, 2019, **53**(15), 8553–8562, DOI: [10.1021/acs.est.9b01609](https://doi.org/10.1021/acs.est.9b01609).
- R. Kaur, B. M. Hudson, J. Draper, D. J. Tantillo and C. Anastasio, Aqueous Reactions of Organic Triplet Excited States with Atmospheric Alkenes, *Atmos. Chem. Phys.*, 2019, **19**(7), 5021–5032, DOI: [10.5194/acp-19-5021-2019](https://doi.org/10.5194/acp-19-5021-2019).
- S. Canonica, Oxidation of Aquatic Organic Contaminants Induced by Excited Triplet States, *Chimia*, 2007, **61**(10), 641, DOI: [10.2533/chimia.2007.641](https://doi.org/10.2533/chimia.2007.641).
- S. Canonica, B. Hellrung, P. Müller and J. Wirz, Aqueous Oxidation of Phenylurea Herbicides by Triplet Aromatic Ketones, *Environ. Sci. Technol.*, 2006, **40**(21), 6636–6641, DOI: [10.1021/es0611238](https://doi.org/10.1021/es0611238).
- M. Minella, L. Rapa, L. Carena, M. Pazzi, V. Maurino, C. Minero, M. Brigante and D. Vione, An Experimental Methodology to Measure the Reaction Rate Constants of Processes Sensitised by the Triplet State of 4-Carboxybenzophenone as a Proxy of the Triplet States of Chromophoric Dissolved Organic Matter, under Steady-State Irradiation Conditions, *Environ. Sci.: Processes Impacts*, 2018, **20**(7), 1007–1019, DOI: [10.1039/C8EM00155C](https://doi.org/10.1039/C8EM00155C).
- D. Vione, M. Minella, V. Maurino and C. Minero, Indirect Photochemistry in Sunlit Surface Waters: Photoinduced Production of Reactive Transient Species, *Chem.–Eur. J.*, 2014, **20**(34), 10590–10606, DOI: [10.1002/chem.201400413](https://doi.org/10.1002/chem.201400413).
- S. Gligorovski, R. Strekowski, S. Barbati and D. Vione, Environmental Implications of Hydroxyl Radicals ($^{\bullet}OH$), *Chem. Rev.*, 2015, **115**(24), 13051–13092, DOI: [10.1021/cr500310b](https://doi.org/10.1021/cr500310b).
- D. Stone, L. K. Whalley and D. E. Heard, Tropospheric OH and HO₂ Radicals: Field Measurements and Model Comparisons, *Chem. Soc. Rev.*, 2012, **41**(19), 6348–6404, DOI: [10.1039/C2CS35140D](https://doi.org/10.1039/C2CS35140D).
- L. Ma, C. Guzman, C. Niedek, T. Tran, Q. Zhang and C. Anastasio, Kinetics and Mass Yields of Aqueous Secondary Organic Aerosol from Highly Substituted Phenols Reacting with a Triplet Excited State, *Environ. Sci. Technol.*, 2021, **55**(9), 5772–5781, DOI: [10.1021/acs.est.1c00575](https://doi.org/10.1021/acs.est.1c00575).
- S. Arciva, C. Niedek, C. Mavis, M. Yoon, M. E. Sanchez, Q. Zhang and C. Anastasio, Aqueous $^{\bullet}OH$ Oxidation of Highly Substituted Phenols as a Source of Secondary



- Organic Aerosol, *Environ. Sci. Technol.*, 2022, **56**(14), 9959–9967, DOI: [10.1021/acs.est.2c02225](https://doi.org/10.1021/acs.est.2c02225).
- 17 L. Yu, J. Smith, A. Laskin, K. M. George, C. Anastasio, J. Laskin, A. M. Dillner and Q. Zhang, Molecular Transformations of Phenolic SOA during Photochemical Aging in the Aqueous Phase: Competition among Oligomerization, Functionalization, and Fragmentation, *Atmos. Chem. Phys.*, 2016, **16**(7), 4511–4527, DOI: [10.5194/acp-16-4511-2016](https://doi.org/10.5194/acp-16-4511-2016).
- 18 N. K. Richards-Henderson, A. T. Pham, B. B. Kirk and C. Anastasio, Secondary Organic Aerosol from Aqueous Reactions of Green Leaf Volatiles with Organic Triplet Excited States and Singlet Molecular Oxygen, *Environ. Sci. Technol.*, 2015, **49**(1), 268–276, DOI: [10.1021/es503656m](https://doi.org/10.1021/es503656m).
- 19 R. Kaur and C. Anastasio, First Measurements of Organic Triplet Excited States in Atmospheric Waters, *Environ. Sci. Technol.*, 2018, **52**(9), 5218–5226, DOI: [10.1021/acs.est.7b06699](https://doi.org/10.1021/acs.est.7b06699).
- 20 L. Ma, R. Worland, W. Jiang, C. Niedek, C. Guzman, K. J. Bein, Q. Zhang and C. Anastasio, Predicting Photooxidant Concentrations in Aerosol Liquid Water Based on Laboratory Extracts of Ambient Particles, *Atmos. Chem. Phys.*, 2023, **23**(15), 8805–8821, DOI: [10.5194/acp-23-8805-2023](https://doi.org/10.5194/acp-23-8805-2023).
- 21 E. R. Graber and Y. Rudich, Atmospheric HULIS: How Humic-like Are They? A Comprehensive and Critical Review, *Atmos. Chem. Phys.*, 2006, 729–753.
- 22 C. Baduel, D. Voisin and J.-L. Jaffrezo, Seasonal Variations of Concentrations and Optical Properties of Water Soluble HULIS Collected in Urban Environments, *Atmos. Chem. Phys.*, 2010, **10**(9), 4085–4095, DOI: [10.5194/acp-10-4085-2010](https://doi.org/10.5194/acp-10-4085-2010).
- 23 C. Baduel, D. Voisin and J. L. Jaffrezo, Comparison of Analytical Methods for Humic Like Substances (HULIS) Measurements in Atmospheric Particles, *Atmos. Chem. Phys.*, 2009, **9**(16), 5949–5962, DOI: [10.5194/acp-9-5949-2009](https://doi.org/10.5194/acp-9-5949-2009).
- 24 C. Zou, M. Li, T. Cao, M. Zhu, X. Fan, S. Peng, J. Song, B. Jiang, W. Jia, C. Yu, H. Song, Z. Yu, J. Li, G. Zhang and P. Peng, Comparison of Solid Phase Extraction Methods for the Measurement of Humic-like Substances (HULIS) in Atmospheric Particles, *Atmos. Environ.*, 2020, **225**, 117370, DOI: [10.1016/j.atmosenv.2020.117370](https://doi.org/10.1016/j.atmosenv.2020.117370).
- 25 T. Zhang, S. Huang, D. Wang, J. Sun, Q. Zhang, H. Xu, S. S. Hang Ho, J. Cao and Z. Shen, Seasonal and Diurnal Variation of PM_{2.5} HULIS over Xi'an in Northwest China: Optical Properties, Chemical Functional Group, and Relationship with Reactive Oxygen Species (ROS), *Atmos. Environ.*, 2022, **268**, 118782, DOI: [10.1016/j.atmosenv.2021.118782](https://doi.org/10.1016/j.atmosenv.2021.118782).
- 26 Z. Ye, Q. Li, S. Ma, Q. Zhou, Y. Gu, Y. Su, Y. Chen, H. Chen, J. Wang and X. Ge, Summertime Day-Night Differences of PM_{2.5} Components (Inorganic Ions, OC, EC, WSOC, WSON, HULIS, and PAHs) in Changzhou, China, *Atmosphere*, 2017, **8**(10), 189, DOI: [10.3390/atmos8100189](https://doi.org/10.3390/atmos8100189).
- 27 H.-M. Lee, S. P. Lee, Y. Li, J. Z. Yu, J. Y. Kim, Y. P. Kim and J. Y. Lee, Characterization of Seasonal Difference of HULIS-C Sources from Water Soluble PM_{2.5} in Seoul, Korea: Probing Secondary Processes, *Aerosol Air Qual. Res.*, 2020, **21**(2), 200233, DOI: [10.4209/aaqr.2020.05.0233](https://doi.org/10.4209/aaqr.2020.05.0233).
- 28 J. Tan, L. Zhang, X. Zhou, J. Duan, Y. Li, J. Hu and K. He, Chemical Characteristics and Source Apportionment of PM_{2.5} in Lanzhou, China, *Sci. Total Environ.*, 2017, **601–602**, 1743–1752, DOI: [10.1016/j.scitotenv.2017.06.050](https://doi.org/10.1016/j.scitotenv.2017.06.050).
- 29 X. Li, J. Han, P. K. Hopke, J. Hu, Q. Shu, Q. Chang and Q. Ying, Quantifying Primary and Secondary Humic-like Substances in Urban Aerosol Based on Emission Source Characterization and a Source-Oriented Air Quality Model, *Atmos. Chem. Phys.*, 2019, **19**(4), 2327–2341, DOI: [10.5194/acp-19-2327-2019](https://doi.org/10.5194/acp-19-2327-2019).
- 30 B. Y. Kuang, P. Lin, X. H. H. Huang and J. Z. Yu, Sources of Humic-like Substances in the Pearl River Delta, China: Positive Matrix Factorization Analysis of PM_{2.5} Major Components and Source Markers, *Atmos. Chem. Phys.*, 2015, **15**(4), 1995–2008, DOI: [10.5194/acp-15-1995-2015](https://doi.org/10.5194/acp-15-1995-2015).
- 31 G. Kiss, M. Gángó, E. Horváth, B. Eck-Varanka, K. Labancz and N. Kováts, Assessment of Ecotoxicity of Atmospheric Humic-like Substances Using the Vibrio Fischeri Bioluminescence Inhibition Bioassay, *Atmos. Environ.*, 2021, **261**, 118561, DOI: [10.1016/j.atmosenv.2021.118561](https://doi.org/10.1016/j.atmosenv.2021.118561).
- 32 P. Lin, X.-F. Huang, L.-Y. He and J. Zhen Yu, Abundance and Size Distribution of HULIS in Ambient Aerosols at a Rural Site in South China, *J. Aerosol Sci.*, 2010, **41**(1), 74–87, DOI: [10.1016/j.jaerosci.2009.09.001](https://doi.org/10.1016/j.jaerosci.2009.09.001).
- 33 V. Kumar, P. Rajput and A. Goel, Atmospheric Abundance of HULIS during Wintertime in Indo-Gangetic Plain: Impact of Biomass Burning Emissions, *J. Atmos. Chem.*, 2018, **75**(4), 385–398, DOI: [10.1007/s10874-018-9381-4](https://doi.org/10.1007/s10874-018-9381-4).
- 34 Y. Wang, M. Hu, P. Lin, Q. Guo, Z. Wu, M. Li, L. Zeng, Y. Song, L. Zeng, Y. Wu, S. Guo, X. Huang and L. He, Molecular Characterization of Nitrogen-Containing Organic Compounds in Humic-like Substances Emitted from Straw Residue Burning, *Environ. Sci. Technol.*, 2017, **51**(11), 5951–5961, DOI: [10.1021/acs.est.7b00248](https://doi.org/10.1021/acs.est.7b00248).
- 35 Q. T. Nguyen, T. B. Kristensen, A. M. K. Hansen, H. Skov, R. Bossi, A. Massling, L. L. Sørensen, M. Bilde, M. Glasius and J. K. Nøjgaard, Characterization of Humic-like Substances in Arctic Aerosols, *J. Geophys. Res.: Atmos.*, 2014, **119**(8), 5011–5027, DOI: [10.1002/2013JD020144](https://doi.org/10.1002/2013JD020144).
- 36 S. Canonica, U. Jans, K. Stemmler and J. Hoigne, Transformation Kinetics of Phenols in Water: Photosensitization by Dissolved Natural Organic Material and Aromatic Ketones, *Environ. Sci. Technol.*, 1995, **29**(7), 1822–1831.
- 37 J. Mack and J. R. Bolton, Photochemistry of Nitrite and Nitrate in Aqueous Solution: A Review, *J. Photochem. Photobiol., A*, 1999, **128**(1), 1–13, DOI: [10.1016/S1010-6030\(99\)00155-0](https://doi.org/10.1016/S1010-6030(99)00155-0).
- 38 P. L. Brezonik and J. Fulkerson-Brekken, Nitrate-Induced Photolysis in Natural Waters: Controls on Concentrations of Hydroxyl Radical Photo-Intermediates by Natural Scavenging Agents, *Environ. Sci. Technol.*, 1998, **32**(19), 3004–3010, DOI: [10.1021/es9802908](https://doi.org/10.1021/es9802908).



- 39 K. B. Benedict, A. S. McFall and C. Anastasio, Quantum Yield of Nitrite from the Photolysis of Aqueous Nitrate above 300 Nm, *Environ. Sci. Technol.*, 2017, **51**(8), 4387–4395, DOI: [10.1021/acs.est.6b06370](https://doi.org/10.1021/acs.est.6b06370).
- 40 M. Gen, Z. Liang, R. Zhang, B. R. G. Mabato and C. K. Chan, Particulate Nitrate Photolysis in the Atmosphere, *Environ. Sci.: Atmos.*, 2022, **2**(2), 111–127, DOI: [10.1039/D1EA00087J](https://doi.org/10.1039/D1EA00087J).
- 41 S. Goldstein, D. Aschengrau, Y. Diamant and J. Rabani, Photolysis of Aqueous H₂O₂: Quantum Yield and Applications for Polychromatic UV Actinometry in Photoreactors, *Environ. Sci. Technol.*, 2007, **41**(21), 7486–7490, DOI: [10.1021/es071379t](https://doi.org/10.1021/es071379t).
- 42 R. Zellner, M. Exner and H. Herrmann, Absolute OH Quantum Yields in the Laser Photolysis of Nitrate, Nitrite and Dissolved H₂O₂ at 308 and 351 Nm in the Temperature Range 278–353 K, *J. Atmos. Chem.*, 1990, **10**(4), 411–425, DOI: [10.1007/BF00115783](https://doi.org/10.1007/BF00115783).
- 43 Y. B. Lim, Y. Tan, M. J. Perri, S. P. Seitzinger and B. J. Turpin, Aqueous Chemistry and Its Role in Secondary Organic Aerosol (SOA) Formation, *Atmos. Chem. Phys.*, 2010, **10**(21), 10521–10539, DOI: [10.5194/acp-10-10521-2010](https://doi.org/10.5194/acp-10-10521-2010).
- 44 C. C. Winterbourn, Toxicity of Iron and Hydrogen Peroxide: The Fenton Reaction, *Toxicol. Lett.*, 1995, **82–83**, 969–974, DOI: [10.1016/0378-4274\(95\)03532-X](https://doi.org/10.1016/0378-4274(95)03532-X).
- 45 W. P. Kwan and B. M. Voelker, Decomposition of Hydrogen Peroxide and Organic Compounds in the Presence of Dissolved Iron and Ferrihydrite, *Environ. Sci. Technol.*, 2002, **36**(7), 1467–1476, DOI: [10.1021/es011109p](https://doi.org/10.1021/es011109p).
- 46 R. A. Floyd and C. A. Lewis, Hydroxyl Free Radical Formation from Hydrogen Peroxide by Ferrous Iron-Nucleotide Complexes, *Biochemistry*, 1983, **22**(11), 2645–2649, DOI: [10.1021/bi00280a008](https://doi.org/10.1021/bi00280a008).
- 47 L. Deguillaume, M. Leriche, K. Desboeufs, G. Mailhot, C. George and N. Chaumerliac, Transition Metals in Atmospheric Liquid Phases: Sources, Reactivity, and Sensitive Parameters, *Chem. Rev.*, 2005, **105**(9), 3388–3431, DOI: [10.1021/cr040649c](https://doi.org/10.1021/cr040649c).
- 48 L. Deguillaume, M. Leriche and N. Chaumerliac, Impact of Radical versus Non-Radical Pathway in the Fenton Chemistry on the Iron Redox Cycle in Clouds, *Chemosphere*, 2005, **60**(5), 718–724, DOI: [10.1016/j.chemosphere.2005.03.052](https://doi.org/10.1016/j.chemosphere.2005.03.052).
- 49 X. Zhou, A. J. Davis, D. J. Kieber, W. C. Keene, J. R. Maben, H. Maring, E. E. Dahl, M. A. Izaguirre, R. Sander and L. Smoydzyn, Photochemical Production of Hydroxyl Radical and Hydroperoxides in Water Extracts of Nascent Marine Aerosols Produced by Bursting Bubbles from Sargasso Seawater, *Geophys. Res. Lett.*, 2008, **35**(20), DOI: [10.1029/2008GL035418](https://doi.org/10.1029/2008GL035418).
- 50 C. Anastasio and A. L. Jordan, Photoformation of Hydroxyl Radical and Hydrogen Peroxide in Aerosol Particles from Alert, Nunavut: Implications for Aerosol and Snowpack Chemistry in the Arctic, *Atmos. Environ.*, 2004, **38**(8), 1153–1166, DOI: [10.1016/j.atmosenv.2003.11.016](https://doi.org/10.1016/j.atmosenv.2003.11.016).
- 51 C. Anastasio and J. T. Newberg, Sources and Sinks of Hydroxyl Radical in Sea-Salt Particles, *J. Geophys. Res.: Atmos.*, 2007, **112**(D10), DOI: [10.1029/2006JD008061](https://doi.org/10.1029/2006JD008061).
- 52 R. Kaur and C. Anastasio, Light Absorption and the Photoformation of Hydroxyl Radical and Singlet Oxygen in Fog Waters, *Atmos. Environ.*, 2017, **164**, 387–397, DOI: [10.1016/j.atmosenv.2017.06.006](https://doi.org/10.1016/j.atmosenv.2017.06.006).
- 53 R. Kaur, J. R. Labins, S. S. Helbock, W. Jiang, K. J. Bein, Q. Zhang and C. Anastasio, Photooxidants from Brown Carbon and Other Chromophores in Illuminated Particle Extracts, *Atmos. Chem. Phys.*, 2019, **19**(9), 6579–6594, DOI: [10.5194/acp-19-6579-2019](https://doi.org/10.5194/acp-19-6579-2019).
- 54 J. V. Trueblood, M. R. Alves, D. Power, M. V. Santander, R. E. Cochran, K. A. Prather and V. H. Grassian, Shedding Light on Photosensitized Reactions within Marine-Relevant Organic Thin Films, *ACS Earth Space Chem.*, 2019, **3**(8), 1614–1623, DOI: [10.1021/acsearthspacechem.9b00066](https://doi.org/10.1021/acsearthspacechem.9b00066).
- 55 M. Roveretto, M. Li, N. Hayeck, M. Brüggemann, C. Emmelin, S. Perrier and C. George, Real-Time Detection of Gas-Phase Organohalogenes from Aqueous Photochemistry Using Orbitrap Mass Spectrometry, *ACS Earth Space Chem.*, 2019, **3**(3), 329–334, DOI: [10.1021/acsearthspacechem.8b00209](https://doi.org/10.1021/acsearthspacechem.8b00209).
- 56 T. Felber, T. Schaefer, L. He and H. Herrmann, Aromatic Carbonyl and Nitro Compounds as Photosensitizers and Their Photophysical Properties in the Tropospheric Aqueous Phase, *J. Phys. Chem. A*, 2021, **125**(23), 5078–5095, DOI: [10.1021/acs.jpca.1c03503](https://doi.org/10.1021/acs.jpca.1c03503).
- 57 P. Corral Arroyo, T. Bartels-Rausch, P. A. Alpert, S. Dumas, S. Perrier, C. George and M. Ammann, Particle-Phase Photosensitized Radical Production and Aerosol Aging, *Environ. Sci. Technol.*, 2018, **52**(14), 7680–7688, DOI: [10.1021/acs.est.8b00329](https://doi.org/10.1021/acs.est.8b00329).
- 58 B. R. G. Mabato, Y. Lyu, Y. Ji, Y. J. Li, D. D. Huang, X. Li, T. Nah, C. H. Lam and C. K. Chan, Aqueous Secondary Organic Aerosol Formation from the Direct Photosensitized Oxidation of Vanillin in the Absence and Presence of Ammonium Nitrate, *Atmos. Chem. Phys.*, 2022, **22**(1), 273–293, DOI: [10.5194/acp-22-273-2022](https://doi.org/10.5194/acp-22-273-2022).
- 59 W. Li, P. Ge, M. Chen, J. Tang, M. Cao, Y. Cui, K. Hu and D. Nie, Tracers from Biomass Burning Emissions and Identification of Biomass Burning, *Atmosphere*, 2021, **12**(11), 1401, DOI: [10.3390/atmos12111401](https://doi.org/10.3390/atmos12111401).
- 60 B. R. T. Simoneit, Biomass Burning — a Review of Organic Tracers for Smoke from Incomplete Combustion, *Appl. Geochem.*, 2002, **17**(3), 129–162, DOI: [10.1016/S0883-2927\(01\)00061-0](https://doi.org/10.1016/S0883-2927(01)00061-0).
- 61 M. R. bin Abas, B. R. T. Simoneit, V. Elias, J. A. Cabral and J. N. Cardoso, Composition of Higher Molecular Weight Organic Matter in Smoke Aerosol from Biomass Combustion in Amazonia, *Chemosphere*, 1995, **30**(5), 995–1015, DOI: [10.1016/0045-6535\(94\)00442-W](https://doi.org/10.1016/0045-6535(94)00442-W).
- 62 W. Li, J. Wang, L. Qi, W. Yu, D. Nie, S. Shi, C. Gu, X. Ge and M. Chen, Molecular Characterization of Biomass Burning Tracer Compounds in Fine Particles in Nanjing, China,



- Atmos. Environ.*, 2020, **240**, 117837, DOI: [10.1016/j.atmosenv.2020.117837](https://doi.org/10.1016/j.atmosenv.2020.117837).
- 63 D. R. Oros and B. R. T. Simoneit, Identification and Emission Factors of Molecular Tracers in Organic Aerosols from Biomass Burning Part 1. Temperate Climate Conifers, *Appl. Geochem.*, 2001, 1513–1544.
- 64 A. Bianco, M. Passananti, H. Perroux, G. Voyard, C. Mouchel-Vallon, N. Chaumerliac, G. Mailhot, L. Deguillaume and M. Brigante, A Better Understanding of Hydroxyl Radical Photochemical Sources in Cloud Waters Collected at the Puy de Dôme Station – Experimental *versus* Modelled Formation Rates, *Atmos. Chem. Phys.*, 2015, **15**(16), 9191–9202, DOI: [10.5194/acp-15-9191-2015](https://doi.org/10.5194/acp-15-9191-2015).
- 65 L. J. S. Borlaza, S. Weber, G. Uzu, V. Jacob, T. Cañete, S. Micallef, C. Trébuchon, R. Slama, O. Favez and J.-L. Jaffrezo, Disparities in Particulate Matter (PM₁₀) Origins and Oxidative Potential at a City Scale (Grenoble, France) – Part 1: Source Apportionment at Three Neighbouring Sites, *Atmos. Chem. Phys.*, 2021, **21**(7), 5415–5437, DOI: [10.5194/acp-21-5415-2021](https://doi.org/10.5194/acp-21-5415-2021).
- 66 Y. Chen, N. Li, X. Li, Y. Tao, S. Luo, Z. Zhao, S. Ma, H. Huang, Y. Chen, Z. Ye and X. Ge, Secondary Organic Aerosol Formation from 3C*-Initiated Oxidation of 4-Ethylguaicol in Atmospheric Aqueous-Phase, *Sci. Total Environ.*, 2020, **723**, 137953, DOI: [10.1016/j.scitotenv.2020.137953](https://doi.org/10.1016/j.scitotenv.2020.137953).
- 67 S. Canonica and M. Freiburghaus, Electron-Rich Phenols for Probing the Photochemical Reactivity of Freshwaters, *Environ. Sci. Technol.*, 2001, **35**(4), 690–695, DOI: [10.1021/es0011360](https://doi.org/10.1021/es0011360).
- 68 Q. Chen, Z. Mu, L. Xu, M. Wang, J. Wang, M. Shan, X. Fan, J. Song, Y. Wang, P. Lin and L. Du, Triplet-State Organic Matter in Atmospheric Aerosols: Formation Characteristics and Potential Effects on Aerosol Aging, *Atmos. Environ.*, 2021, **252**, 118343, DOI: [10.1016/j.atmosenv.2021.118343](https://doi.org/10.1016/j.atmosenv.2021.118343).
- 69 L. Ma, R. Worland, T. Tran and C. Anastasio, Evaluation of Probes to Measure Oxidizing Organic Triplet Excited States in Aerosol Liquid Water, *Environ. Sci. Technol.*, 2023, **57**(15), 6052–6062, DOI: [10.1021/acs.est.2c09672](https://doi.org/10.1021/acs.est.2c09672).
- 70 T. Charbouillot, M. Brigante, G. Mailhot, P. R. Maddigapu, C. Minero and D. Vione, Performance and Selectivity of the Terephthalic Acid Probe for OH as a Function of Temperature, PH and Composition of Atmospherically Relevant Aqueous Media, *J. Photochem. Photobiol., A*, 2011, **222**(1), 70–76, DOI: [10.1016/j.jphotochem.2011.05.003](https://doi.org/10.1016/j.jphotochem.2011.05.003).
- 71 G. Žerjav, A. Albrecht, I. Vovk and A. Pintar, Revisiting Terephthalic Acid and Coumarin as Probes for Photoluminescent Determination of Hydroxyl Radical Formation Rate in Heterogeneous Photocatalysis, *Appl. Catal., A*, 2020, **598**, 117566, DOI: [10.1016/j.apcata.2020.117566](https://doi.org/10.1016/j.apcata.2020.117566).
- 72 X. Wei, T. Ji, S. Zhang, Z. Xue, C. Lou, M. Zhang, S. Zhao, H. Liu, X. Guo, B. Yang and J. Chen, Cerium-Terephthalic Acid Metal-Organic Frameworks for Ratiometric Fluorescence Detecting and Scavenging[•]OH from Fuel Combustion Gas, *J. Hazard. Mater.*, 2022, **439**, 129603, DOI: [10.1016/j.jhazmat.2022.129603](https://doi.org/10.1016/j.jhazmat.2022.129603).
- 73 J. Chen, Y. Si, Y. Liu, S. Wang, S. Wang, Y. Zhang, B. Yang, Z. Zhang and S. Zhang, Starch-Regulated Copper-Terephthalic Acid as a PH/Hydrogen Peroxide Simultaneous-Responsive Fluorescent Probe for Lysosome Imaging, *Dalton Trans.*, 2019, **48**(34), 13017–13025, DOI: [10.1039/C9DT02193K](https://doi.org/10.1039/C9DT02193K).
- 74 Y. Nosaka, S. Komori, K. Yawata, T. Hirakawa and A. Y. Nosaka, Photocatalytic [•]OH Radical Formation in TiO₂ Aqueous Suspension Studied by Several Detection Methods, *Phys. Chem. Chem. Phys.*, 2003, **5**(20), 4731–4735, DOI: [10.1039/B307433A](https://doi.org/10.1039/B307433A).
- 75 Y. Jing and B. P. Chaplin, Mechanistic Study of the Validity of Using Hydroxyl Radical Probes To Characterize Electrochemical Advanced Oxidation Processes, *Environ. Sci. Technol.*, 2017, **51**(4), 2355–2365, DOI: [10.1021/acs.est.6b05513](https://doi.org/10.1021/acs.est.6b05513).
- 76 T. Hirakawa, K. Yawata and Y. Nosaka, Photocatalytic Reactivity for O₂^{•-} and OH Radical Formation in Anatase and Rutile TiO₂ Suspension as the Effect of H₂O₂ Addition, *Appl. Catal., A*, 2007, **325**(1), 105–111, DOI: [10.1016/j.apcata.2007.03.015](https://doi.org/10.1016/j.apcata.2007.03.015).
- 77 J. Liu, G. Lagger, P. Tacchini and H. H. Girault, Generation of OH Radicals at Palladium Oxide Nanoparticle Modified Electrodes, and Scavenging by Fluorescent Probes and Antioxidants, *J. Electroanal. Chem.*, 2008, **619–620**, 131–136, DOI: [10.1016/j.jelechem.2008.03.017](https://doi.org/10.1016/j.jelechem.2008.03.017).
- 78 Q. Chen, Y. Miyazaki, K. Kawamura, K. Matsumoto, S. Coburn, R. Volkamer, Y. Iwamoto, S. Kagami, Y. Deng, S. Ogawa, S. Ramasamy, S. Kato, A. Ida, Y. Kajii and M. Mochida, Characterization of Chromophoric Water-Soluble Organic Matter in Urban, Forest, and Marine Aerosols by HR-ToF-AMS Analysis and Excitation–Emission Matrix Spectroscopy, *Environ. Sci. Technol.*, 2016, **50**(19), 10351–10360, DOI: [10.1021/acs.est.6b01643](https://doi.org/10.1021/acs.est.6b01643).
- 79 X. Fan, S. Wei, M. Zhu, J. Song and P. Peng, Comprehensive Characterization of Humic-like Substances in Smoke PM_{2.5} Emitted from the Combustion of Biomass Materials and Fossil Fuels, *Atmos. Chem. Phys.*, 2016, **16**(20), 13321–13340, DOI: [10.5194/acp-16-13321-2016](https://doi.org/10.5194/acp-16-13321-2016).
- 80 Z. Han, M. Xiao, F. Yue, Y. Yi and K. M. G. Mostofa, Seasonal Variations of Dissolved Organic Matter by Fluorescent Analysis in a Typical River Catchment in Northern China, *Water*, 2021, **13**(4), 494, DOI: [10.3390/w13040494](https://doi.org/10.3390/w13040494).
- 81 Y. Ma, R. Mao and S. Li, Hydrological Seasonality Largely Contributes to Riverine Dissolved Organic Matter Chemical Composition: Insights from EEM-PARAFAC and Optical Indicators, *J. Hydrol.*, 2021, **595**, 125993, DOI: [10.1016/j.jhydrol.2021.125993](https://doi.org/10.1016/j.jhydrol.2021.125993).
- 82 G. Wu, P. Fu, K. Ram, J. Song, Q. Chen, K. Kawamura, X. Wan, S. Kang, X. Wang, A. Laskin and Z. Cong, Fluorescence Characteristics of Water-Soluble Organic Carbon in Atmospheric Aerosol[☆], *Environ. Pollut.*, 2021, **268**, 115906, DOI: [10.1016/j.envpol.2020.115906](https://doi.org/10.1016/j.envpol.2020.115906).



- 83 P. Lin, N. Bluvshstein, Y. Rudich, S. A. Nizkorodov, J. Laskin and A. Laskin, Molecular Chemistry of Atmospheric Brown Carbon Inferred from a Nationwide Biomass Burning Event, *Environ. Sci. Technol.*, 2017, **51**(20), 11561–11570, DOI: [10.1021/acs.est.7b02276](https://doi.org/10.1021/acs.est.7b02276).
- 84 A. Rana, S. Dey, P. Rawat, A. Mukherjee, J. Mao, S. Jia, P. S. Khillare, A. K. Yadav and S. Sarkar, Optical Properties of Aerosol Brown Carbon (BrC) in the Eastern Indo-Gangetic Plain, *Sci. Total Environ.*, 2020, **716**, 137102, DOI: [10.1016/j.scitotenv.2020.137102](https://doi.org/10.1016/j.scitotenv.2020.137102).
- 85 Y. Lyu, Y. H. Lam, Y. Li, N. Borduas-Dedekind and T. Nah, Seasonal Variations in the Production of Singlet Oxygen and Organic Triplet Excited States in Aqueous PM_{2.5} in Hong Kong SAR, South China, *Atmos. Chem. Phys.*, 2023, **23**(16), 9245–9263, DOI: [10.5194/acp-23-9245-2023](https://doi.org/10.5194/acp-23-9245-2023).
- 86 W. Jiang, L. Ma, C. Niedeck, C. Anastasio and Q. Zhang, Chemical and Light-Absorption Properties of Water-Soluble Organic Aerosols in Northern California and Photooxidant Production by Brown Carbon Components, *ACS Earth Space Chem.*, 2023, **7**(5), 1107–1119, DOI: [10.1021/acsearthspacechem.3c00022](https://doi.org/10.1021/acsearthspacechem.3c00022).
- 87 L. Ma, R. Worland, L. Heinlein, C. Guzman, W. Jiang, C. Niedeck, K. J. Bein, Q. Zhang and C. Anastasio, Seasonal Variations in Photooxidant Formation and Light Absorption in Aqueous Extracts of Ambient Particles, *Atmos. Chem. Phys.*, 2024, **24**(1), 1–21, DOI: [10.5194/acp-24-1-2024](https://doi.org/10.5194/acp-24-1-2024).
- 88 K. Takeda, H. Takedoi, S. Yamaji, K. Ohta and H. Sakugawa, Determination of Hydroxyl Radical Photoproduction Rates in Natural Waters, *Anal. Sci.*, 2004, **20**(1), 153–158, DOI: [10.2116/analsci.20.153](https://doi.org/10.2116/analsci.20.153).
- 89 K. Mopper and X. Zhou, Hydroxyl Radical Photoproduction in the Sea and Its Potential Impact on Marine Processes, *Science*, 1990, **250**(4981), 661–664, DOI: [10.1126/science.250.4981.661](https://doi.org/10.1126/science.250.4981.661).
- 90 T. Arakaki and B. C. Faust, Sources, Sinks, and Mechanisms of Hydroxyl Radical ([•]OH) Photoproduction and Consumption in Authentic Acidic Continental Cloud Waters from Whiteface Mountain, New York: The Role of the Fe(r) (r = II, III) Photochemical Cycle, *J. Geophys. Res.: Atmos.*, 1998, **103**(D3), 3487–3504, DOI: [10.1029/97JD02795](https://doi.org/10.1029/97JD02795).
- 91 M. Cao, W. Li, P. Ge, M. Chen and J. Wang, Seasonal Variations and Potential Sources of Biomass Burning Tracers in Particulate Matter in Nanjing Aerosols during 2017–2018, *Chemosphere*, 2022, **303**, 135015, DOI: [10.1016/j.chemosphere.2022.135015](https://doi.org/10.1016/j.chemosphere.2022.135015).
- 92 Y. J. Li, D. D. Huang, H. Y. Cheung, A. K. Y. Lee and C. K. Chan, Aqueous-Phase Photochemical Oxidation and Direct Photolysis of Vanillin – a Model Compound of Methoxy Phenols from Biomass Burning, *Atmos. Chem. Phys.*, 2014, **14**(6), 2871–2885, DOI: [10.5194/acp-14-2871-2014](https://doi.org/10.5194/acp-14-2871-2014).
- 93 C. Anastasio and K. G. McGregor, Chemistry of Fog Waters in California's Central Valley: 1. *In Situ* Photoformation of Hydroxyl Radical and Singlet Molecular Oxygen, *Atmos. Environ.*, 2001, **35**(6), 1079–1089, DOI: [10.1016/S1352-2310\(00\)00281-8](https://doi.org/10.1016/S1352-2310(00)00281-8).
- 94 T. Arakaki, Y. Kuroki, K. Okada, Y. Nakama, H. Ikota, M. Kinjo, T. Higuchi, M. Uehara and A. Tanahara, Chemical Composition and Photochemical Formation of Hydroxyl Radicals in Aqueous Extracts of Aerosol Particles Collected in Okinawa, Japan, *Atmos. Environ.*, 2006, **40**(25), 4764–4774, DOI: [10.1016/j.atmosenv.2006.04.035](https://doi.org/10.1016/j.atmosenv.2006.04.035).
- 95 R.-J. Huang, L. Yang, J. Shen, W. Yuan, Y. Gong, H. Ni, J. Duan, J. Yan, H. Huang, Q. You and Y. J. Li, Chromophoric Fingerprinting of Brown Carbon from Residential Biomass Burning, *Environ. Sci. Technol. Lett.*, 2022, **9**(2), 102–111, DOI: [10.1021/acs.estlett.1c00837](https://doi.org/10.1021/acs.estlett.1c00837).
- 96 D.-L. Nguyen, H. Czech, S. M. Pieber, J. Schnelle-Kreis, M. Steinbacher, J. Orasche, S. Henne, O. B. Popovicheva, G. Abbaszade, G. Engling, N. Bukowiecki, N.-A. Nguyen, X.-A. Nguyen and R. Zimmermann, Carbonaceous Aerosol Composition in Air Masses Influenced by Large-Scale Biomass Burning: A Case Study in Northwestern Vietnam, *Atmos. Chem. Phys.*, 2021, **21**(10), 8293–8312, DOI: [10.5194/acp-21-8293-2021](https://doi.org/10.5194/acp-21-8293-2021).
- 97 J. Yang, T. Zhou, Y. Lyu, B. R. G. Mabato, J. C.-H. Lam, C. K. Chan and T. Nah, Effects of Copper on Chemical Kinetics and Brown Carbon Formation in the Aqueous [•]OH Oxidation of Phenolic Compounds, *Environ. Sci.: Processes Impacts*, 2024, DOI: [10.1039/D4EM00191E](https://doi.org/10.1039/D4EM00191E).
- 98 W. Yuan, R.-J. Huang, L. Yang, J. Guo, Z. Chen, J. Duan, T. Wang, H. Ni, Y. Han, Y. Li, Q. Chen, Y. Chen, T. Hoffmann and C. O'Dowd, Characterization of the Light-Absorbing Properties, Chromophore Composition and Sources of Brown Carbon Aerosol in Xi'an, Northwestern China, *Atmos. Chem. Phys.*, 2020, **20**(8), 5129–5144, DOI: [10.5194/acp-20-5129-2020](https://doi.org/10.5194/acp-20-5129-2020).
- 99 M. A. J. Harrison, S. Barra, D. Borghesi, D. Vione, C. Arsene and R. Iulian Olariu, Nitrated Phenols in the Atmosphere: A Review, *Atmos. Environ.*, 2005, **39**(2), 231–248, DOI: [10.1016/j.atmosenv.2004.09.044](https://doi.org/10.1016/j.atmosenv.2004.09.044).
- 100 S. Yan, J. Sun, H. Sha, Q. Li, J. Nie, J. Zou, C. Chu and W. Song, Microheterogeneous Distribution of Hydroxyl Radicals in Illuminated Dissolved Organic Matter Solutions, *Environ. Sci. Technol.*, 2021, **55**(15), 10524–10533, DOI: [10.1021/acs.est.1c03346](https://doi.org/10.1021/acs.est.1c03346).

